LETTERS
PUBLISHED ONLINE: 14 DECEMBER 2015 | DOI: 10.1038/NCLIMATE2888
nature climate change

Implications for climate sensitivity from the response to individual forcings

Kate Marvel[1,2]*, Gavin A. Schmidt[2]*, Ron L. Miller[1,2]* and Larissa S. Nazarenko[2,3]

Climate sensitivity to doubled CO_2 is a widely used metric for the large-scale response to external forcing. Climate models predict a wide range for two commonly used definitions: the transient climate response (TCR: the warming after 70 years of CO_2 concentrations that rise at 1% per year), and the equilibrium climate sensitivity (ECS: the equilibrium temperature change following a doubling of CO_2 concentrations). Many observational data sets have been used to constrain these values, including temperature trends over the recent past[1–6], inferences from palaeoclimate[7,8] and process-based constraints from the modern satellite era[9,10]. However, as the IPCC recently reported[11], different classes of observational constraints produce somewhat incongruent ranges. Here we show that climate sensitivity estimates derived from recent observations must account for the efficacy of each forcing active during the historical period. When we use single-forcing experiments to estimate these efficacies and calculate climate sensitivity from the observed twentieth-century warming, our estimates of both TCR and ECS are revised upwards compared to previous studies, improving the consistency with independent constraints.

The concept of radiative forcing is used to compare the effects of different physical drivers on the Earth's energy budget. Two forcing agents that produce a similar radiative imbalance might be expected to initiate similar feedbacks and have the same global mean temperature response[12]. However, there can be variations in the size and type of feedbacks engendered by a specific forcing[13], mainly due to geographical variations in the forcing magnitude. These variations can be characterized by an efficacy that scales for the differences in temperature response. Forcings that project more strongly on the Northern Hemisphere, land or polar regions are systematically more effective at changing temperatures than an equivalent amount of CO_2, whose forcing is more uniformly distributed throughout the globe[13,14]. The converse is true for forcings localized in the Southern Hemisphere or ocean regions.

Some published constraints on ECS, particularly from the Last Glacial Maximum, have attempted to incorporate forcing efficacies into their assessments[15,16], although none of the recently published constraints derived from modern trends have fully done so[3–6]. However, ECS does not provide the information on transient, short-term climate impacts that TCR reflects. It therefore remains unclear to what extent efficacies derived for equilibrium results are applicable to transient situations where ocean heat uptake plays an important role[17–20].

An analysis of transient simulations with interactive aerosols[21] indicated that the combination of anthropogenic aerosols, ozone, and land-use change affect global temperature trends more efficiently than does CO_2 forcing alone (that is, the efficacy of the combination is greater than unity). However, the specific contributions of individual forcings have thus far remained obscure. In this paper, we use a large suite of single-forcing simulations to estimate the impact of combined forcings in transient simulations for the historical period and show that proper consideration of the resulting efficacies implies that previously derived constraints on ECS and TCR should be revised upwards.

For the Coupled Model Intercomparison Project, Phase 5 (CMIP5), the NASA Goddard Institute for Space Studies (GISS) modelling group performed 'historical' simulations using model version GISS-E2-R spanning 1850–2005, driven by estimates of relevant natural and external forcings[22]. Multiple simulations over the same time period using single forcings or combinations of forcings were also submitted to the CMIP5 'historicalMisc' archive, including simulations forced by only well-mixed greenhouse gases (GHGs), anthropogenic aerosols (AA), ozone (Oz), solar variations (Sl), volcanoes (Vl), or land-use changes (LU). These unique ensembles allow us to replicate climate sensitivity calculations in a 'perfect model' framework, in which we have all the information we need to determine transient and equilibrium sensitivities using previously published methods, which can be compared to the actual TCR (1.4 °C) and ECS (2.3 °C) of the GISS-E2-R model[23,24].

TCR depends on the transient changes in global mean temperature ΔT and radiative forcing ΔF. To calculate ECS, we also require estimates of the rate of ocean heat content (OHC) change ΔQ. We use ΔQ here instead of the more conventional TOA imbalances[25] to restrict our analysis to observables that have been used in previous analyses. Both ΔQ and ΔT are readily estimated from model output (see Supplementary Methods). However, there are several different definitions of radiative forcing[13,25], and we use two methods to capture different aspects of the planetary response to external agents. First, we calculate the annual-mean, global instantaneous radiative forcing (iRF) as the initial radiative flux change, evaluated at the tropopause in an attempt to anticipate the effect of rapid stratospheric adjustments[26], for each year 1900–2005 (Supplementary Methods). Second, we calculate the effective radiative forcing (ERF), which incorporates changes in the troposphere and land surface that are rapid compared to the ocean temperature response, using fixed-SST experiments forced with year-2000 values of each forcing (Supplementary Methods).

We first estimate the climate sensitivities using the instantaneous radiative forcings ΔF, combined with the historical annual global mean temperature anomaly ΔT and ocean heat uptake anomaly ΔQ for each non-overlapping ten-year period beginning with 1906–1915 and ending with 1996–2005 (Supplementary Methods and Supplementary Fig. 1).

[1]Department of Applied Physics and Applied Mathematics, Columbia University, New York, New York 10027, USA. [2]NASA Goddard Institute for Space Studies, New York, New York 10025, USA. [3]Center for Climate Systems Research, Columbia University, New York, New York 10025, USA.
*e-mail: kate.marvel@nasa.gov; gavin.a.schmidt@nasa.gov; ron.l.miller@nasa.gov

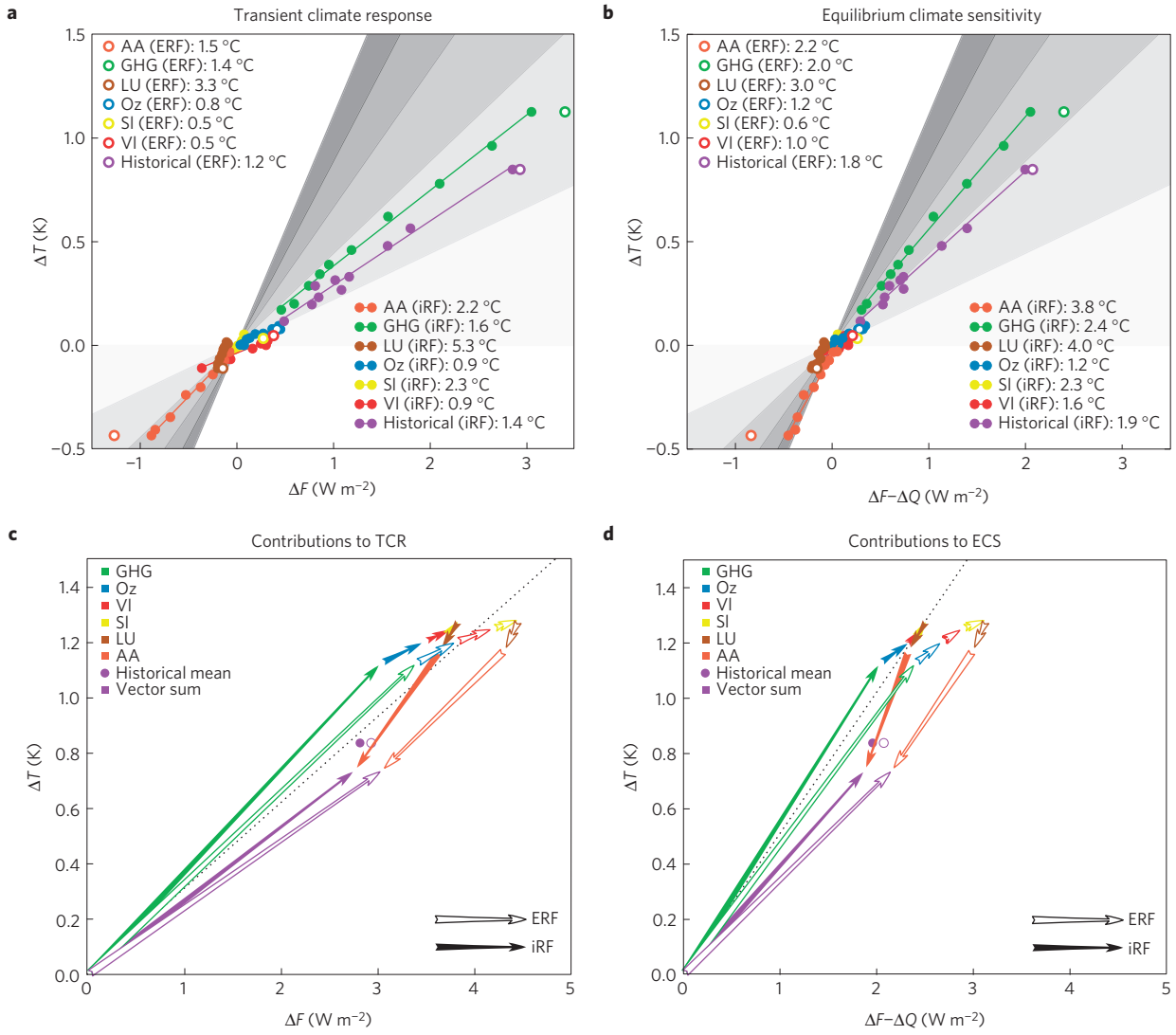

Figure 1 | Model historical and single-forcing transient and equilibrium sensitivities. a, Non-overlapping ensemble average decadal mean changes in temperature and instantaneous radiative forcing for GISS-E2-R single-forcing ensembles (filled circles) (defined with respect to 1850–1859). TCR is calculated from the slope of the best-fit line. Also shown are 1996–2005 temperature changes and effective radiative forcing (open circles). In this case, TCR is the quotient of the temperature and ERF estimates. Following ref. 4, straight grey contours show isolines of TCR from 0 to 4 for the iRF case. **b**, Same, but changes in the rate of ocean heat uptake are subtracted from forcing changes. ECS is calculated from the slope of the best-fit line (for iRF) or from the quotient (for ERF). **c**, 1996–2005 average ΔT and instantaneous (filled arrows) and effective (white arrows) radiative forcing for each single-forcing experiment. The transient climate response for each experiment in each case is the slope of the line. The vector sum of the single-forcing values does not substantially differ from the historical values (circles) and the TCR of the sum and historical experiments is less than that of the GHG-only experiment. The published GISS-E2-R TCR (1.4 °C) is shown as a dashed black line. **d**, Same as **c**, but the *x* axis shows the difference of 1996–2005 average forcing and estimated ocean heat uptake. The slope of each line is the equilibrium climate sensitivity. The published GISS-E2-R ECS (2.3 °C) is shown as a dashed black line.

For each decade, we plot the temperature anomaly versus forcing (for TCR, Fig. 1a) or the difference between forcing and ocean heat uptake anomalies (for ECS, Fig. 1b). Using

$$\Delta F = \lambda_{\mathrm{TCR}} \Delta T; \qquad \Delta F = \lambda_{\mathrm{ECS}} \Delta T + \Delta Q \tag{1}$$

we calculate λ as the slope of the best-fit line in both cases[4]. Using only the first and last decades gives comparable results. The TCR and ECS are then given by

$$\mathrm{TCR} = \frac{F_{2\times \mathrm{CO_2}}}{\lambda_{\mathrm{TCR}}}; \qquad \mathrm{ECS} = \frac{F_{2\times \mathrm{CO_2}}}{\lambda_{\mathrm{ECS}}} \tag{2}$$

where $F_{2\times \mathrm{CO_2}}$ is the model forcing for CO_2 doubling. These linear methods assume that both λ_{ECS} and λ_{TCR} are constant in time, despite evidence[27] that this may result in an underestimate of the 'true' values.

The ratios of single-forcing TCR and ECS to CO_2-only TCR and ECS define transient and equilibrium efficacies, respectively[13]. These are measures of the enhancement (or suppression) of the climate response to the forcing relative to the climate response to CO_2. Supplementary Table 1 lists the transient and equilibrium efficacies calculated from the GISS-E2-R single-forcing runs, along with uncertainties derived from the five-member ensembles for each forcing.

The global mean climate responses to different forcings may differ because of the character of the forcings themselves (such as their geographical or vertical distribution) and because different forcings induce different patterns of surface warming or cooling,

thereby affecting the net top-of-atmosphere radiation imbalance, and thus the ocean heat uptake rate ΔQ. The evolving pattern of temperature change may be incorporated into a global mean framework as an 'ocean heat uptake efficacy'[18]. Our methodology does not differentiate between these two physical mechanisms, and we note that a substantial portion of what we call 'forcing efficacy' may be due to differences between the ocean heat uptake induced by CO_2 forcing and the heat uptake induced by the forcing in question.

In keeping with previous studies[13,14,21,28], we find that aerosols have an enhanced transient climate response by roughly 30% and equilibrium response by 50%. Furthermore, the transient and equilibrium efficacies of ozone and volcanic forcing are significantly less than unity in the perfect model framework; other studies[29,30] have also found that volcanic forcing has a smaller impact on global temperatures than an equivalent change in greenhouse gas forcing. The efficacies for LU and Sl calculated in this framework are uncertain owing to the small changes in these forcing agents over the historical period, although we do find that the best estimates for LU transient and equilibrium efficacy generally exceed unity, probably owing to hemispheric asymmetry and land bias in this forcing.

Previous work[13] found that certain equilibrium efficacies, notably anthropogenic tropospheric aerosols, decrease towards unity when the iRF is replaced by the ERF to incorporate tropospheric adjustments. This raises the possibility that the use of effective, rather than instantaneous radiative forcing, may render the sensitivities from GHG-only and historical simulations more directly comparable. We therefore re-calculate efficacies using the ERFs (open circles in Fig. 1 and Supplementary Fig. 1). Although aerosol transient and equilibrium efficacies are indeed reduced when using ERF (Supplementary Table 1), TCR and ECS calculated from the combined effective radiative forcings within the 'historical' experiment remain biased low compared to the GHG-only values (Fig. 1).

Because the forcings and temperature responses are additive, we can show in a vector plot the relative contributions of each forcing to the discrepancies between sensitivities derived from CO_2-only simulations and those estimated from historical simulations (Fig. 1c,d). This shows clearly that the low sensitivities of the historical runs (compared to values obtained from CO_2-only simulations) result from the higher efficacy of aerosols (when calculated using iRF) and land-use change, along with the lower efficacy of ozone and volcanic responses. Figure 1c,d indicates that many of the forcings over the recent historical period are less effective at changing global temperatures than those that cool the surface. We note that aerosol efficacy when calculated with ERF is compatible with unity; implying that differences between the historical sensitivities and CO_2-only sensitivities are attributable to the other forcings.

Scaling ΔF for each of the single-forcing runs by the relevant efficacy yields sensitivities estimated from the historical runs comparable to those derived from CO_2-only runs (Supplementary Methods and Supplementary Fig. 2); because the forcings and temperatures add linearly, the resulting calculation with the historical all-forcing run scaled by the historical efficacy will also yield the same sensitivity as in the CO_2-only runs.

What are the implications of our estimated forcing efficacies for constraints on sensitivity based on historical observations? Using our perfect model analysis, we can combine the model efficacies with historical forcings and the temperature response to estimate the observed climate sensitivity for comparison to existing calculations. Here, we make no attempt to evaluate the quality of existing observations or their suitability for estimating climate sensitivity; rather, we seek to replicate existing estimates and show how they change once efficacies are taken into account.

Assuming that all forcings have the same transient efficacy as greenhouse gases, and following a previous study[4], the best estimate

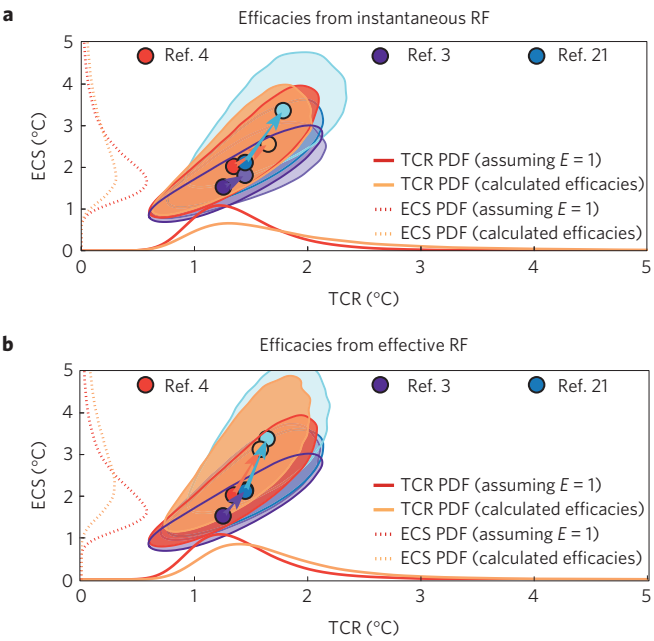

Figure 2 | Sensitivity estimates from observations. a, TCR and ECS best-guess values (circles) and 95% joint confidence intervals (shaded regions). These are first calculated assuming all efficacies = 1 (darker colours) and then incorporating efficacies calculated using iRF. Arrows indicate the revisions in TCR and ECS when efficacies are taken into account. Estimates from three published works[3,4,21] and their revisions are shown. Original (red) and revised (orange) TCR and ECS probability distribution functions calculated using ref. 4 data are shown on the *x* and *y* axes, respectively. **b**, Same, but efficacies are calculated using effective radiative forcing (ERF).

(median) for TCR is 1.3 °C (see Supplementary Methods). Scaling each forcing by our estimates of transient efficacy determined from iRF we obtain a best estimate for TCR of 1.7 °C (Fig. 2a) (1.6 °C if efficacies are detemined from ERF). This scaling simultaneously considers both forcing and ocean heat uptake efficacy. Other estimates of TCR without efficacies[3,21], which differ slightly owing to choices of base period and uncertainty estimates and the aerosol forcing used, are similarly revised upwards when using calculated efficacies (Fig. 2a).

We apply the same reasoning to estimates of ECS. Using an estimate[4] of the rate of recent heat uptake $\Delta Q = 0.65 \pm 0.27$ W m^{-2}, we find, assuming all equilibrium efficacies are unity, a best estimate of ECS = 2.0 °C, comparable to the previous result[4] of 1.9 °C. However, as with TCR, accounting for differences in equilibrium forcing efficacy revises the estimate upwards; our new best estimate (using efficacies derived from the iRF) is 2.6 °C (Fig. 2a). If efficacies are instead calculated from the ERF, the best estimate of ECS is 3.0 °C (Fig. 2b). As for TCR, alternative estimates of ECS are revised upwards when efficacies are taken into account (Fig. 2b).

Estimates of both ECS and TCR are very sensitive to errors and uncertainties in the observations. Differences in the spread and best estimates for ECS and TCR (Supplementary Table 2) will depend on the base periods used, estimates of ocean heat uptake, and on the aerosol forcing and its uncertainty. It is not the goal of this paper to assess different observational estimates. However, we note that in all cases, incorporating differing transient and equilibrium efficacies results in higher estimates for TCR and ECS.

The calculated efficacies used here are based on a single model. To increase confidence in these values it would be necessary to perform the suite of single-forcing experiments with additional models. These experiments were a low priority in CMIP5, and

the historicalMisc archive is sparse. Moreover, very few groups performed comparable calculations of radiative forcings associated with each forcing agent. In cases where forcing is small over the whole historical period (LU, Sl) uncertainty is large. Simulations in which land-use changes or solar forcings are amplified may be necessary to constrain the efficacy of these forcings.

We stress the importance of clearly defining 'radiative forcing'. Although TCR and ECS estimates are revised upwards regardless of the radiative forcing definition used to calculate efficacies, this is attributable to different factors when effective, rather than instantaneous, radiative forcing is used. The major difference is the calculated efficacy of anthropogenic aerosol forcing, which approaches unity when fast tropospheric adjustments are incorporated. Previous studies involving the GISS model[13] found that rapid cloud changes in both hemispheres result from the rapid adjustment to aerosol forcing; effective radiative forcing is thus more hemispherically symmetric than instantaneous aerosol forcing. This increased symmetry may account for the reduced aerosol efficacy when calculated with ERF. However, further study in a multi-model context will be necessary to better constrain the efficacy associated with historical aerosol changes.

GISS ModelE2 is more sensitive to CO_2 alone than it is to the sum of the forcings that were important over the past century. This is largely a result of the low efficacy of ozone and volcanic forcings and the high efficacy of aerosol and LU forcing (which have had a cooling effect over the historical period), although further study is needed to explore model differences in simulating efficacies and to enhance confidence in these estimates. Climate sensitivities estimated from recent observations will therefore be biased low in comparison with CO_2-only simulations owing to an accident of history: when the efficacies of the forcings in the recent historical record are properly taken into account, estimates of TCR and ECS must be revised upwards. Accounting for this results in recent historical estimates for TCR and ECS that are more consistent with constraints based on palaeoclimate data and process-based constraints from modern climatology. Methodologies that attempt to combine independently derived constraints on sensitivity should ensure that such biases are corrected before any synthesis is performed.

Received 11 June 2015; accepted 28 October 2015; published online 14 December 2015; corrected online 10 March 2016

References

1. Forest, C. E., Stone, P. H., Sokolov, A. P., Allen, M. R. & Webster, M. D. Quantifying uncertainties in climate system properties with the use of recent climate observations. *Science* **295,** 113–117 (2002).
2. Forest, C. E., Stone, P. H. & Sokolov, A. P. Estimated PDFs of climate system properties including natural and anthropogenic forcings. *Geophys. Res. Lett.* **33,** L01705 (2006).
3. Lewis, N. & Curry, J. A. The implications for climate sensitivity of AR5 forcing and heat uptake estimates. *Clim. Dynam.* **45,** 1009–1023 (2014).
4. Otto, A. *et al.* Energy budget constraints on climate response. *Nature Geosci.* **6,** 415–416 (2013).
5. Ring, M. J., Lindner, D., Cross, E. F. & Schlesinger, M. E. Causes of the global warming observed since the 19th century. *Atmos. Clim. Sci.* **02,** 401–415 (2012).
6. Aldrin, M. *et al.* Bayesian estimation of climate sensitivity based on a simple climate model fitted to observations of hemispheric temperatures and global ocean heat content. *Environmetrics* **23,** 253–271 (2012).
7. PALAEOSENS Project Members. Making sense of palaeoclimate sensitivity. *Nature* **491,** 683–691 (2012).
8. Hargreaves, J. C., Annan, J. D., Yoshimori, M. & Abe-Ouchi, A. Can the Last Glacial Maximum constrain climate sensitivity? *Geophys. Res. Lett.* **39,** L24702 (2012).
9. Sherwood, S. C., Bony, S. & Dufresne, J. Spread in model climate sensitivity traced to atmospheric convective mixing. *Nature* **505,** 37–42 (2014).
10. Fasullo, J. T. & Trenberth, K. E. A less cloudy future: the role of subtropical subsidence in climate sensitivity. *Science* **338,** 792–794 (2012).
11. Collins, M. *et al.* in *Climate Change 2013: The Physical Science Basis* (eds Stocker, T. F. *et al.*) 1029–1136 (IPCC, Cambridge Univ. Press, 2013).
12. Hansen, J. *et al.* in *Climate Processes and Climate Sensitivity* Vol. 29 (eds Hansen, J. E. & Takahashi, T.) 130–163 (American Geophysical Union, 1984).
13. Hansen, J. E. *et al.* Efficacy of climate forcings. *J. Geophys. Res.* **110,** D18104 (2005).
14. Stuber, N., Ponater, M. & Sausen, R. Why radiative forcing might fail as a predictor of climate change. *Clim. Dynam.* **24,** 497–510 (2005).
15. Köhler, P. *et al.* What caused Earth's temperature variations during the last 800,000 years? Data-based evidence on radiative forcing and constraints on climate sensitivity. *Quat. Sci. Rev.* **29,** 129–145 (2010).
16. Schmittner, A. *et al.* Climate sensitivity estimated from temperature reconstructions of the Last Glacial Maximum. *Science* **334,** 1385–1388 (2011).
17. Rose, B. E., Armour, K. C., Battisti, D. S., Feldl, N. & Koll, D. D. The dependence of transient climate sensitivity and radiative feedbacks on the spatial pattern of ocean heat uptake. *Geophys. Res. Lett.* **41,** 1071–1078 (2014).
18. Winton, M., Takahashi, K. & Held, I. M. Importance of ocean heat uptake efficacy to transient climate change. *J. Clim.* **23,** 2333–2344 (2010).
19. Armour, K. C., Bitz, C. M. & Roe, G. H. Time-varying climate sensitivity from regional feedbacks. *J. Clim.* **26,** 4518–4534 (2013).
20. Kummer, J. R. & Dessler, A. E. The impact of forcing efficacy on the equilibrium climate sensitivity. *Geophys. Res. Lett.* **41,** 3565–3568 (2014).
21. Shindell, D. T. Inhomogeneous forcing and transient climate sensitivity. *Nature Clim. Change* **4,** 274–277 (2014).
22. Miller, R. L. *et al.* CMIP5 historical simulations (1850–2012) with GISS ModelE2. *J. Adv. Model. Earth Syst.* **6,** 441–477 (2014).
23. Nazarenko, L. *et al.* Future climate change under rcp emission scenarios with GISS ModelE2. *J. Adv. Model. Earth Syst.* **7,** 244–267 (2015).
24. Schmidt, G. A. *et al.* Configuration and assessment of the GISS ModelE2 contributions to the CMIP5 archive. *J. Adv. Model. Earth Syst.* **6,** 141–184 (2014).
25. Gregory, J. M. *et al.* A new method for diagnosing radiative forcing and climate sensitivity. *Geophys. Res. Lett.* **31,** L03205 (2004).
26. Hansen, J. E. *et al.* Forcings and chaos in interannual to decadal climate change. *J. Geophys. Res.* **102,** 25679–25720 (1997).
27. Gregory, J. M., Andrews, T. & Good, P. The inconstancy of the transient climate response parameter under increasing CO_2. *Phil. Trans. R. Soc. A* **373,** 20140417 (2015).
28. Shindell, D. & Faluvegi, G. Climate response to regional radiative forcing during the twentieth century. *Nature Geosci.* **2,** 294–300 (2009).
29. Tomassini, L., Reichert, P., Knutti, R., Stocker, T. F. & Borsuk, M. E. Robust bayesian uncertainty analysis of climate system properties using Markov Chain Monte Carlo methods. *J. Clim.* **20,** 1239–1254 (2007).
30. Merlis, T. M., Held, I. M., Stenchikov, G. L., Zeng, F. & Horowitz, L. W. Constraining transient climate sensitivity using coupled climate model simulations of volcanic eruptions. *J. Clim.* **27,** 7781–7795 (2014).

Acknowledgements

Climate modelling at GISS is supported by the NASA Modeling, Analysis and Prediction Program and resources supporting this work were provided by the NASA High-End Computing (HEC) Program through the NASA Center for Climate Simulation (NCCS) at Goddard Space Flight Center. The authors thank D. McNeall and E. Hawkins for advice on figures, and E. Hawkins, J. Gregory, M. Webb, K. Taylor and R. Pincus for helpful discussions.

Author contributions

K.M. and G.A.S. designed the research and wrote the paper, with input from R.L.M. R.L.M. and L.S.N. provided the forcing data. L.S.N. ran the climate model experiments. All authors contributed to the interpretation of the results.

Additional information

Supplementary information is available in the online version of the paper. Reprints and permissions information is available online at www.nature.com/reprints. Correspondence and requests for materials should be addressed to K.M., G.A.S. or R.L.M.

Competing financial interests

The authors declare no competing financial interests.